Changgui Cheng*, Feng Zhang, Yang Li, Ying Chen and Yan Jin

Mathematical Modeling on Deformation Behavior of Solidified Shell in Continuous Slab Casting with Soft Reduction

DOI 10.1515/htmp-2016-0140
Received June 30, 2016; accepted January 21, 2017

Abstract: Based on the calculation results of the two-dimensional unsteady heat transfer model for continuous slab casting with soft reduction process, a coupled thermo-elastic-plastic mathematical model has been developed to study the effects of the reduction amount and solid phase fraction in slab centerline on the deformation behavior of solidification shell in this paper. The calculated results show that the displacement along thickness direction of slab changes little in width center region of slab when the reduction amount keeps constant, then it increases and a peak of displacement appears in 0.075 m whose distance is far from the slab narrow face, finally, it decreases severely near the narrow face of slab. When the solid phase fraction is the same, the displacement of solidification shell toward to the width and thickness direction of slab increases with the increasing of reduction amount. When the solid phase fraction is 0.3, the reduction amount in reduction subzone is 0.15 mm and 0.25 mm, respectively, the effective reduction efficiency decreases from 0.463 to 0.436. When the total reduction amount is 5 mm, the solid phase fraction varies from 0.3 to 0.7, the accumulated displacement of solidification front increases from 0.238 mm to 0.805 mm, the reduction efficiency decreases from 0.46 to 0.32.

Keywords: mathematical model, slab, soft reduction, solidification shell, deformation behavior

Introduction

Serious centerline segregation of slab can destroy the mechanical properties of finished products, and the negative effects on the performance of the final products cannot be eliminated even through the rolling or forging program is adopted in following process [1]. The mechanical soft reduction (MSR) technology is usually adopted in continuous casting for controlling the centerline segregation of slab [2]; however, the application effect of MSR is sometimes not ideal, this may be related to the inappropriate process parameters of MSR, such as the soft reduction zone, the soft reduction ratio, the total reduction amount and so on [3]. In order to improve the application effect of MSR in continuous slab casting, metallurgical workers have made considerable optimizations for the model of MSR. Stetina Josef et al. [4] used a 3D thermal model for the optimum setting, the shrinkage of material was controlled with the setting of the reduction profile, and the wear of the rolls was considered when setting the profile with rollers. Luo Sen et al. [5] developed a theoretical model for determining the optimum soft reduction zone for continuous slab casting, and all optimum soft reduction positions of different solute elements should be included in order to eliminate the centerline segregation effectively. Based on the heat transfer and solidification model for simulating two-phase zones by coupled multiple alloys during continuous slab casting process and the soft reduction theory, Zhang Qi et al. [6] and Han Zhiwei et al. [7] have made some optimization for dynamic soft reduction control.

The solidification front of slab is pushed toward to the center with MSR process, it can offset the shrinkage of the steel liquid near the solidification end, and the negative suction force in the liquid core can be eliminated, then the centerline segregation can be controlled. Thus, the reasonable soft reduction amount is particularly important. Wu Menghuai et al. [8] developed a two-phase columnar solidification model to study the principle of MSR and found that the MSR efficiency depends not only on the reduction amount along the slab thickness direction but also strongly on the deformation behavior in the longitudinal (casting) direction. Gan Yong et al. [9] studied the liquid core reduction behavior in thin slab by means of the coupled thermo mechanical finite element model with the modified Lagrange large

***Corresponding author: Changgui Cheng,** The State Key Laboratory of Refractories and Metallurgy, Wuhan University of Science and Technology, Wuhan 430081, China, E-mail: ccghlx@wust.edu.cn
Feng Zhang, Yang Li, Ying Chen, Yan Jin, The State Key Laboratory of Refractories and Metallurgy, Wuhan University of Science and Technology, Wuhan 430081, China

deformation. Lu Zhouwei et al. [10] established a 3D coupled elastic-plastic-thermo mechanical model with deformation and analyzed the effects of the reduction ratio and the shell thickness on the stress and strain of the slab. Chen Qian et al. [11] studied the collapsing of solidification front under the different solid phase fraction in slab center, molten steel static pressure, deformation amount of MSR and transition cavity shape by using of the finite element analysis method, and concluded that the origin of the collapse phenomenon is the instability of narrow side shell with MSR. Luo Sen et al. [12] described the deformation behavior of strand with MSR and analyzed the effects of process parameters of MSR on the deformation behavior of strand. These researches are helpful to understand the migration behavior of the solidified front of slab with MSR.

In this paper, a thermo-elastic-plastic coupled stress model is established based on the calculated results of the two-dimensional unsteady heat transfer model of slab. The effects of soft reduction zone, soft reduction amount, and solid phase fraction in slab centerline on the deformation behavior of solidification front have been analyzed, and the reduction efficiency of MSR has been also gained under the different condition. These works should be beneficial to optimize the process parameters of MSR and eliminate the centerline segregation of slab

Mathematical model description

In this paper, the casting size of slab is 1,950 mm × 230 mm, the casting temperature is 1,539.4 °C, the casting speed is 1.2 m/min, and the steel grade is Q235B. The solid phase fraction in slab centerline corresponding to the soft reduction zone is 0.3 to 0.7, the total soft reduction amount is about 4–6 mm, considering the central symmetry of slab, the total reduction amount of one side for slab is 2–3 mm, the total soft reduction can be divided into some subzones, the soft reduction amount in some reduction subzones is chosen as 0.15 mm, 0.20 mm and 0.25 mm in this paper, respectively.

Assumptions and equation of heat transfer model

To establish the two-dimensional unsteady heat transfer model of slab, some assumptions are made for simplification: (1) The heat transfer along the casting direction is neglected. (2) The temperatures of liquid steel in meniscus are equivalent to the casting temperature. (3) The effect of liquid steel convection in liquid pool is considered in the determination of thermal conductivity. (4) The thermal physical parameters of steel are considered as the function of temperature.

According to energy conservation law and above assumptions, the heat transfer mathematical equation of continuous slab casting can be derived as follows [13]:

$$\rho c\frac{\partial T}{\partial t}=\frac{\partial}{\partial x}(\lambda\frac{\partial T}{\partial x})+\frac{\partial}{\partial y}(\lambda\frac{\partial T}{\partial y})+L_s \tag{1}$$

where ρ is density of steel, kg/m^3, c is specific heat capacity of steel, J/(kg·°C), T is temperature, °C, λ is thermal conductivity of steel, J/(m·s·°C), t is time, s, x and y are coordinates, m, Ls is latent heat, kJ/kg.

Assumptions and equation of thermo-elastic-plastic coupled model

In order to establish the thermal-elastic-plastic coupled model, some assumptions have been adopted in this paper. (1) The effect of creep on the stress and strain of slab is ignored, (2) The steel is isotropic, and the mechanical properties of strand are changed with the variation of slab temperature, (3) The stress originated from the slab straightening and misalignment arc is ignored, (4) The local solidification shrinkage of the solidified shell is smaller than the reduction amount, and it is therefore ignored, (5) the reduction amount is realized by controlling the displacement of the boundary in model, and the bulging of the wide side is ignored.

The slab deformation with MSR process is the thermo-elastic-plastic deformation, and it has the characteristics of geometric nonlinearity and physical nonlinearity. The physical nonlinearity can be represented by the model constitutive relation, the thermo-elastic-plastic constitutive equations established by the incremental theory are given as follows:

$$\{d\varepsilon\}=\{d\varepsilon_e\}+\{d\varepsilon_p\}+\{d\varepsilon_T\}+\{d\varepsilon_{e,T}\} \tag{2}$$

where $\{d\varepsilon\}$ is total strain increment, $\{d\varepsilon_\varepsilon\}$ is elastic strain increment, $\{d\varepsilon_p\}$ is plastic strain increment, $\{d\varepsilon_T\}$ is thermal strain increment, $\{d\varepsilon_{\varepsilon,T}\}$ is strain increment which is caused by material properties change with different temperature.

When the solidified shell is in elastic state, the stress–strain relationship satisfies Hooks Law, and is given as follows:

$$\{d\sigma\} = [D_e] \cdot \{d\varepsilon_e\} \tag{3}$$

where $[D_e]$ is elastic matrix.

$$[D_e] = \begin{bmatrix} \lambda + 2G & \lambda & 0 \\ \lambda & \lambda + 2G & 0 \\ 0 & 0 & G \end{bmatrix} \tag{4}$$

where λ is Lame coefficient, G is shear modulus of materials, Pa.

When the solidified shell is in plastic state, it should follow the yield criterion, the flow rule and the strengthen law. According to Misses yield criterion, the new yield criterion is given in formula (5).

$$\bar{\sigma} = H \cdot (\int d\overline{\varepsilon_p}) \tag{5}$$

And, the increment form of stress is given in formula (6),

$$d\bar{\sigma} = H \cdot d\overline{\varepsilon_p} \tag{6}$$

where $\overline{\varepsilon_p}$ is equivalent strain.

According to flow criterion, the increment of stress–strain is given as follows,

$$d\{\sigma\} = [D_{ep}] \cdot (\{d\varepsilon\} - \{\Delta\varepsilon^T\}) + d(\sigma_0) \tag{7}$$

$$\{\Delta\varepsilon^T\} = \{d\varepsilon_T\} + \{d\varepsilon_{e,T}\} \tag{8}$$

$$d\{\sigma_0\} = \frac{[D_e] \cdot \frac{\partial\bar{\sigma}}{\partial\{\sigma\}} \cdot \frac{\partial H}{\partial T} dT}{H + \left\{\frac{\partial\bar{\sigma}}{\partial\{\sigma\}}\right\}^T \cdot [D_e] \cdot \frac{\partial\bar{\sigma}}{\partial\{\sigma\}}} \tag{9}$$

where $[D_{ep}]$ is elastic-plastic matrix, H is the equivalent plastic modulus of the material, Pa.

According to Hardening criterion, the dynamic enhancement is adopted in this paper, the size of the yield surface is remained constantly and only changed in plane style in the plastic deformation process.

Initial conditions and boundary conditions

Initial condition of heat transfer model: the temperature in meniscus area is 1,539.4 °C.

Boundary conditions of heat transfer model: the heat flux along the casting direction in the mold is:

$$q_m = 2670000 - B\sqrt{t_m} \tag{10}$$

where q_m is heat flux of mold, J/(m^2·s), B is coefficient which is determined by relations of the average heat flux and instantaneous heat flux in mold, t_m is the slab residence time in the mold.

The heat flux in the secondary cooling zone is:

$$q_s = h_s \cdot (T_{sur} - T_w) + k \cdot \varepsilon\sigma \left[\left(\frac{T_{sur} + 273}{100} \right)^4 - \left(\frac{T_a + 273}{100} \right)^4 \right] \tag{11}$$

where q_s is heat flux, J/(m^2·s), T_{sur} is the slab surface temperature, °C, T_w is cooling water temperature, °C, k is correction factor, ε is steel emissivity, σ is Boltzmann constant, T_a is ambient temperature, °C, h_s is heat transfer coefficient in different secondary cooling subzone, J/(m^2·s·°C), which is defined as formula (12):

$$h_S = 5840 \times W^{0.451} \times \left(1 - 7.5 \times 10^{-3} \times T_w\right) \tag{12}$$

where W is volume density of spraying water, l/(cm^2.min).

Initial conditions of thermo-elastic-plastic coupled model: the initial displacement of node is 0, it is replaced by next step calculated results, the temperature loads in nodes are updated by results of heat transfer model, and the stress loads of last step in nodes are included in the next step calculation.

Boundary condition of thermo-elastic-plastic coupled model: the symmetric displacement boundary conditions applied to the symmetry, namely, the Y direction (thickness direction of slab) displacement of nodes in X-axis (the X direction is the width direction of slab) is 0, the X direction displacement of nodes in Y-axis is 0, and the soft reduction amount is applied to the surface of the model, and it is controlled by the boundary line of model.

The indirect coupling method is adopted in paper, the temperature load is applied in calculated unit, then the thermo-mechanical analysis is made, and displacement and stress of nodes are calculated, then the procedures are made repeatedly. In order to ensure the calculation convergence of thermo-elastic-plastic coupled model, the convergence tolerance of the stress is taken as 0.005, the convergence tolerance of displacement is taken as 0.01.

Results and analysis

Effect of soft reduction amount on deformation behavior of solidification shell

When the solid phase fraction in slab centerline is 0.3, the temperature distribution in quarter cross-section of

slab calculated by heat transfer model is shown in Figure 1, the reduction amount in reduction subzone is 0.15 mm, 0.20 mm and 0.25 mm, respectively, the corresponding displacement nephogram along the width direction of slab under the different reduction amounts are shown in Figure 2.

From Figure 2, it can be seen that the displacement along width direction of slab increases with increasing of the soft reduction amount, which is consistent with deformation behavior of slab with MSR process. For the temperature in slab corner is uneven in Figure 1, the corresponding displacement in slab corner is also uneven in Figure 2. In order to determine the displacement in the same place under different soft reduction amounts, the line whose distance is 65 mm far from width surface of slab is chosen as reference, the displacements along width direction of slab in different places have been shown in Figure 3.

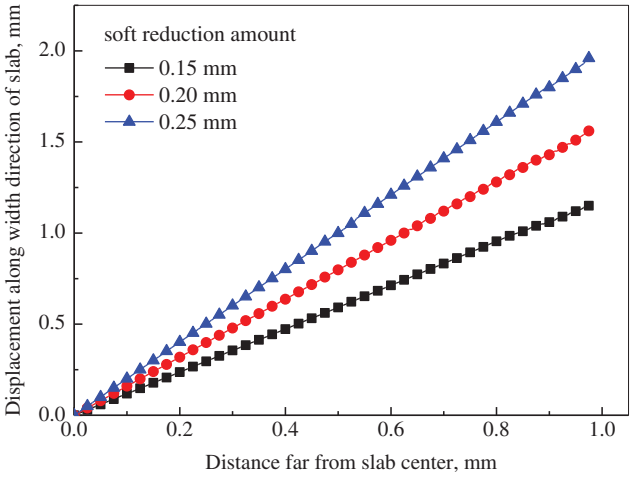

Figure 3: Relationship between displacement along width direction of slab and distance far from slab center.

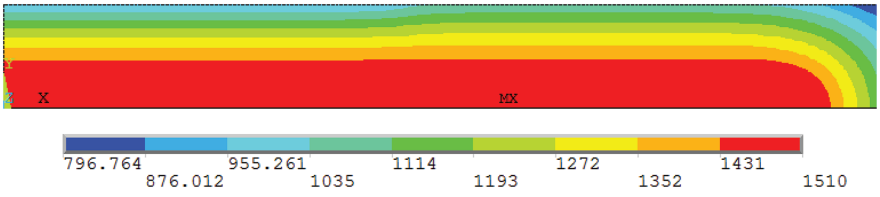

Figure 1: Temperature distribution in quarter cross-section of slab.

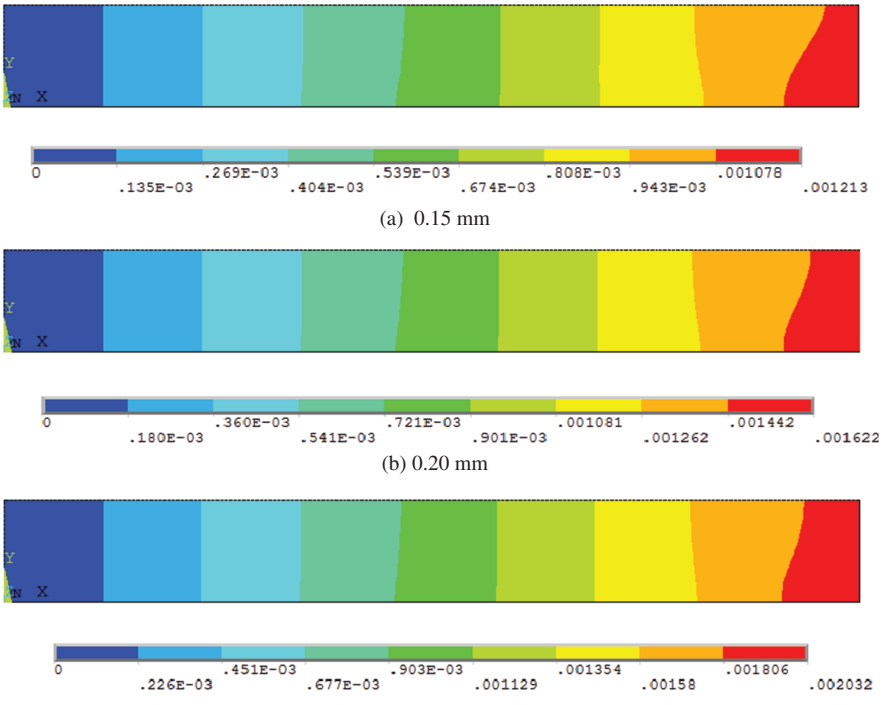

Figure 2: Displacement nephogram along width direction of slab under different reduction amounts.

From Figure 3, it can be seen that the displacement along slab width direction on different place increases linearly with increasing of the soft reduction amount and the distance far from slab center, this is due to the fact that the narrow side of slab is not constraint, it extends easily along width direction of slab when MSR is adopted.

When the solid phase fraction in slab centerline is 0.3, the reduction amount in reduction subzone is 0.15 mm, 0.20 mm and 0.25 mm, respectively, the corresponding displacement nephogram along the thickness direction of slab under different reduction amounts are shown in Figure 4. The displacements along thickness direction of slab whose distance is 65 mm far from width surface of slab are shown in Figure 5.

From Figure 5, it can be seen that displacement along thickness direction of slab changes little in width center area under the same reduction amount, then it increases and a peak of deformation displacement appears in 0.075 m whose distance is far from the slab narrow face, finally, it decreases severely near the narrow face of slab. The deformation phenomenon of solidification shell is related to the slab temperature, the temperature near the narrow face of slab is lower, thus, it is not easy to deform, while the temperature is high in the adjacent area of slab narrow face, the solidification shell can be depressed inward to the slab center when the MSR is adopted, the corresponding displacement is larger.

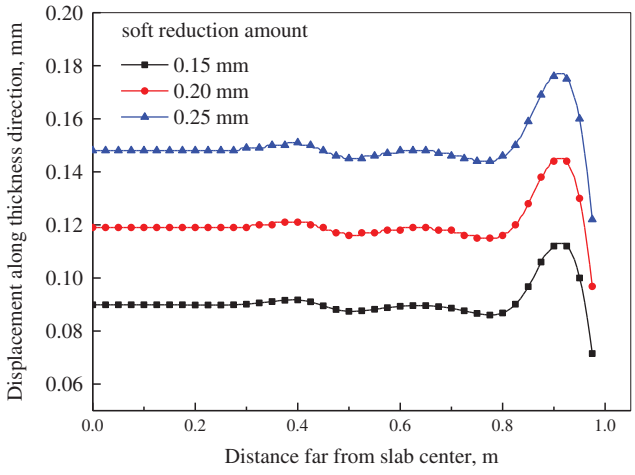

Figure 5: Relationship between displacement along thickness direction of slab and distance far from slab center.

Effect of solid phase fraction in slab centerline on deformation behavior of solidification shell

When the reduction amount is 0.2 mm in reduction subzone, the solid phase fraction in slab centerline is 0.3, 0.4, 0.5, 0.6 and 0.7, respectively, the displacement nephogram along width direction and thickness direction of slab are shown in Figures 6 and 7, respectively.

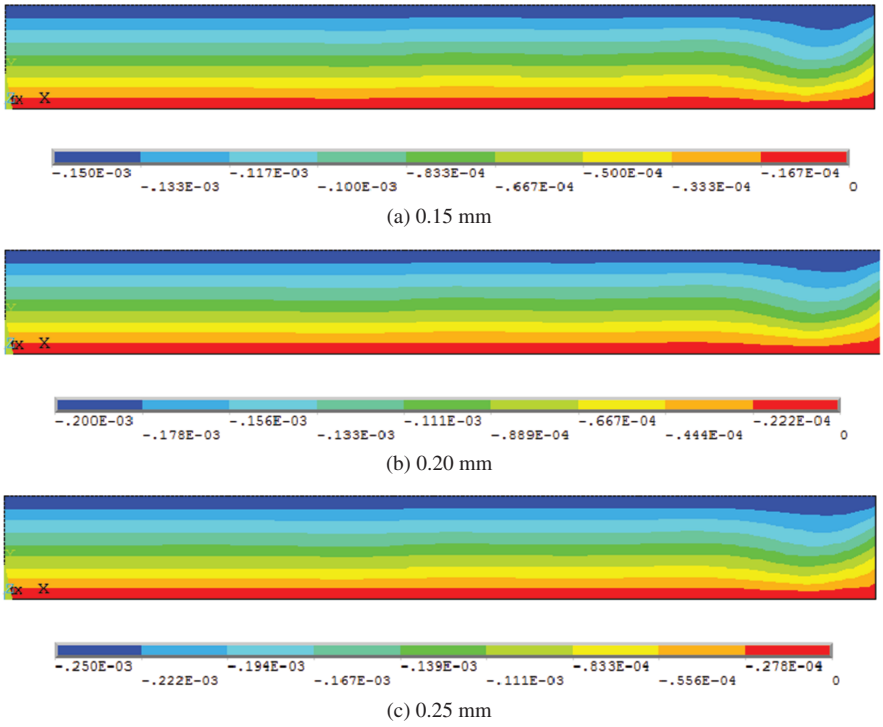

Figure 4: Displacement nephogram along thickness direction of slab under different reduction amounts.

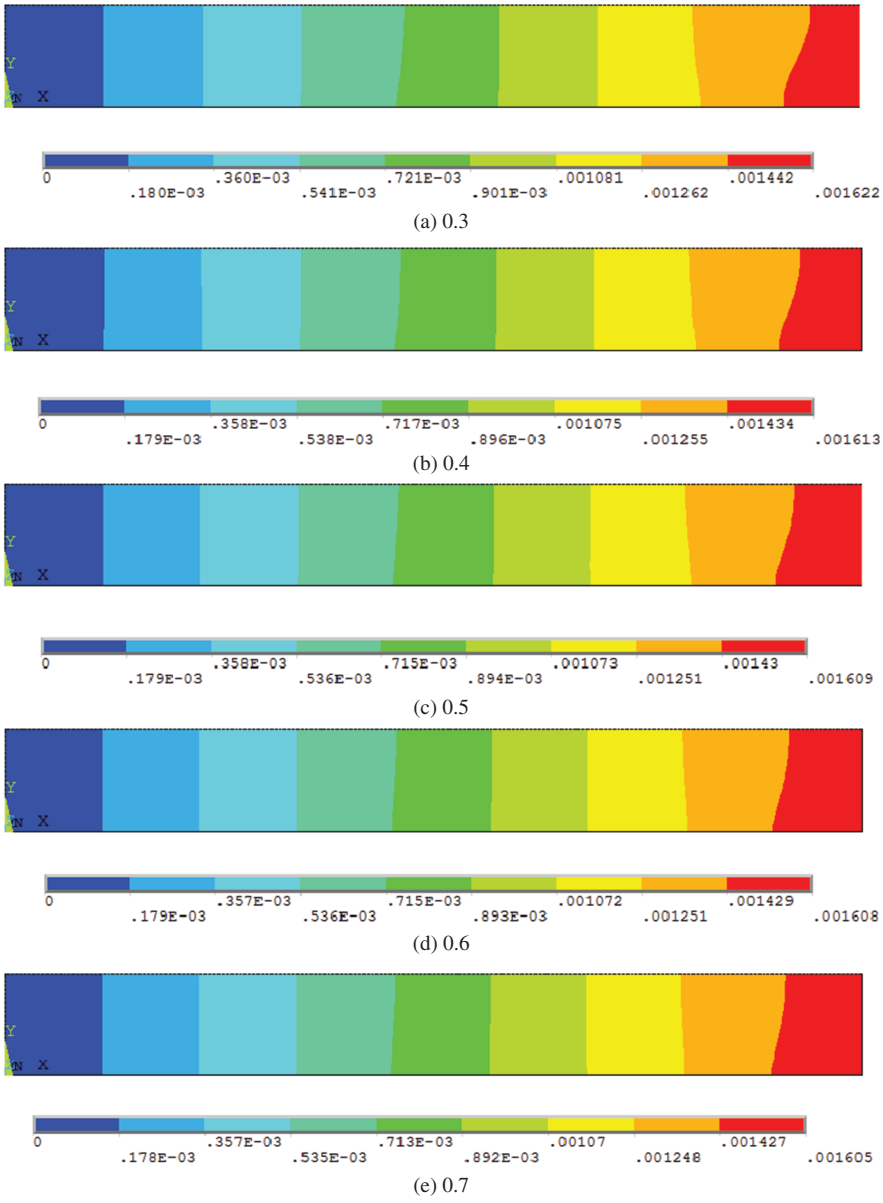

Figure 6: Displacement nephogram along width direction of slab under different solid phase fraction.

From Figure 6, it can be seen that the displacement along width direction of slab changes little with increasing of the solid phase fraction in slab centerline. In order to verify the results, the different reduction amounts are chosen, the place whose distance is far from width surface of slab is 65 mm, the variation law of displacement along width direction of slab is similar, and the variation extent of displacement is little.

From Figure 7, it can be seen that the displacement along thickness direction of slab in the same place decreases with increasing of solid phase fraction. The displacements along thickness direction in place whose distance is 65 mm far from the width surface of slab have been shown as Figure 8.

From Figure 8, it can be seen that the displacement along thickness direction near slab center decreases little with the increasing of solid phase fraction, as the temperature in these region decreases little. The displacement along thickness direction near slab narrow surface varies obviously, this is because that the strength of solidification shell is low when the solid phase fraction is 0.3, then it can be pressed into the liquid steel core of slab.

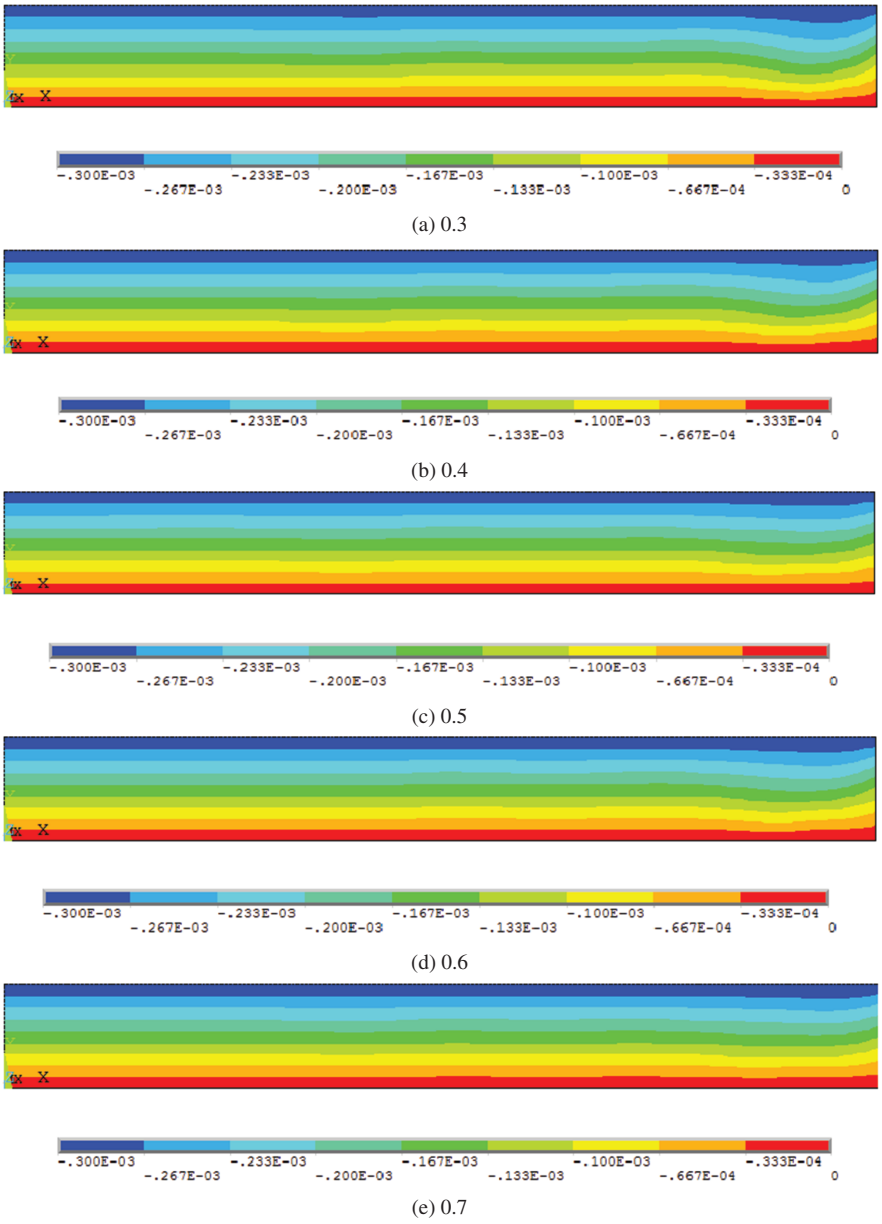

(a) 0.3

(b) 0.4

(c) 0.5

(d) 0.6

(e) 0.7

Figure 7: Displacement nephogram along thickness direction of slab under different solid phase fraction.

Effects of reduction amount on soft reduction efficiency

The soft reduction efficiency has important influence on the control effects of centerline segregation of slab, which is closely related to the displacement of solidification front. The solidification front position of slab has been gained by the heat transfer model, the displacement along thickness direction of slab in different node is determined in Section "Effect of solid phase fraction in slab centerline on deformation behavior of solidification shell", then the average displacement of solidification front can be gained. When the solid phase fraction is 0.3, 0.4, 0.5, 0.6 and 0.7, respectively, the position of solidification front is shown in Figure 9 without MSR process.

When the solid phase fraction is 0.3, the soft reduction amounts in reduction subzone are 0.15 mm, 0.20 mm and 0.25 mm, respectively, the average displacement of solidification front has been given in Table 1.

The calculated formula of soft reduction efficiency is given as follows,

$$\eta = \frac{\Delta h}{\Delta H} \tag{13}$$

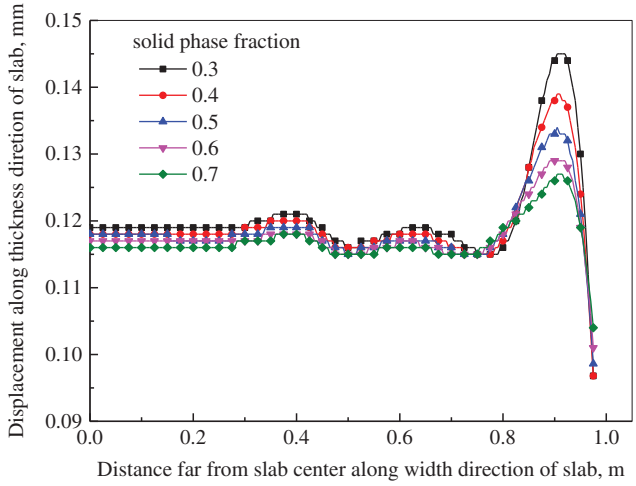

Figure 8: Relationship between displacement along thickness direction of slab and distance far from slab center.

where Δh is reduce of liquid core thickness of slab, ΔH is the reduce of shell thickness which is namely soft reduction amount. η is soft reduction efficiency. The relationship between the soft reduction efficiency and soft reduction amount is shown in Figure 10.

From Figure 10, it can be seen that the soft reduction efficiency decreases from 0.463 to 0.436 with increasing of soft reduction amount. However, the decreasing extent of soft reduction efficiency is not significant, and this is related to the approximate shell strength when the solid phase fraction is the same.

Effects of solid phase fraction on soft reduction efficiency

When the soft reduction amount is 0.2 mm, the solid phase fraction is 03, 0.4, 0.5, 0.6 and 0.7, respectively, the average displacement of solidification front has been given in Table 2. The relationship between the soft reduction efficiency and solid phase fraction is shown in Figure 11.

From Figure 11, it can be seen that the efficiency reduction decreases from 0.44 to 0.22 with increasing of the solid phase fraction. This is because of that the slab temperature decreases with increasing of the solid phase fraction, the slab cannot deform easily, simultaneously, the solidification front of inner arc and external arc of slab are closer, and it hinders the soft reduction behavior, then the reduction efficiency decreases. Meanwhile, the shrinkage of liquid steel in slab center is high when the solid phase fraction in slab centerline is lower, it needs more compensation to eliminate the negative suction force, thus, the soft reduction amount should be larger when the solid phase fraction is lower, and it is smaller when the solid phase fraction is high.

Table 1: Average displacement of solidification front under different soft reduction amount.

Soft reduction amount, mm	0.15	0.2	0.25
Average displacement, mm	0.068	0.088	0.109

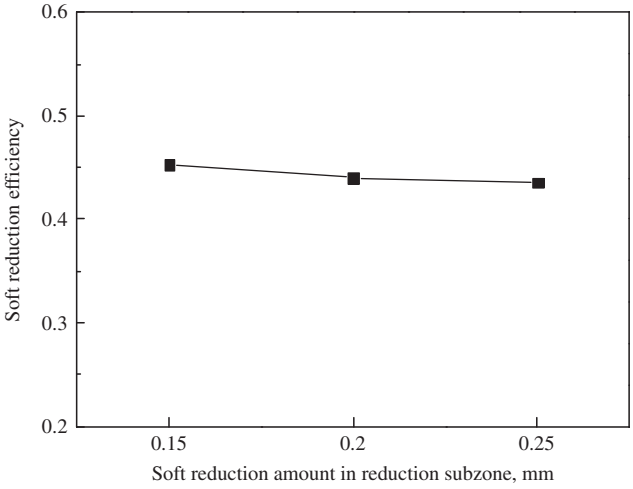

Figure 10: Relationship between the soft reduction efficiency and soft reduction amount.

Table 2: Average displacement of solidification front under different solid phase fraction.

Solid phase fraction	0.3	0.4	0.5	0.6	0.7
Average displacement, mm	0.088	0.073	0.061	0.052	0.044

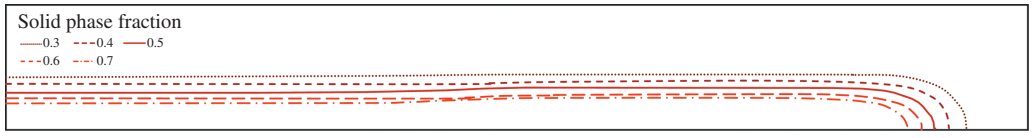

Figure 9: Solidification front position under different solid phase fraction.

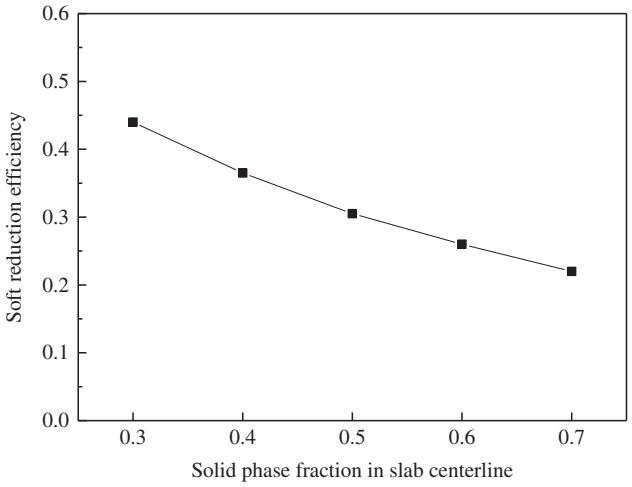

Figure 11: Relationship between the soft reduction efficiency and solid phase fraction in slab centerline.

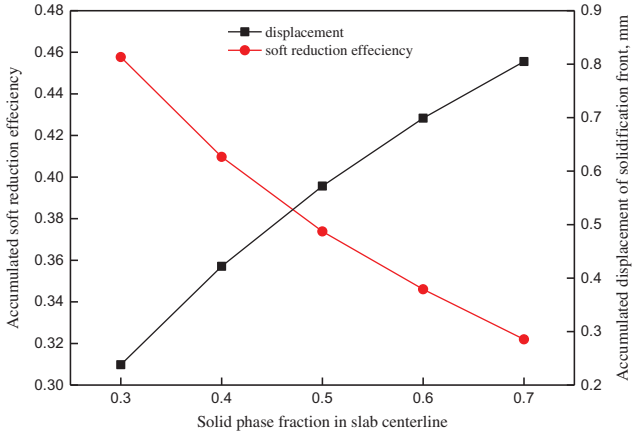

Figure 12: Relationship between the calculated accumulated displacement of solidification front and soft reduction efficiency and solid phase fraction.

Displacement of solidification front under different total soft reduction amount

The above analysis is based on the soft reduction amount in the reduction subzone. When the total soft reduction amount is 5 mm, the soft reduction amount in different subzones follows the distribution rule which the reduction amount in the previous subzone is larger and it is lower in the back subzone, the distribution of soft reduction amount in each subzone is given in Table 3, the average solid phase fraction in subzone is used to represent the position of the soft reduction subzone. The calculated average displacement of solidification front is given in Table 4.

Table 3: Soft reduction amount in different reduction subzone.

Average solid phase fraction	0.3	0.4	0.5	0.6	0.7
Soft reduction amount, mm	0.52	0.51	0.5	0.49	0.48

Table 4: Average displacement of solidification front in different solid phase fraction zone.

Average solid phase fraction	0.3	0.4	0.5	0.6	0.7
Average displacement of solidification front, mm	0.238	0.184	0.150	0.127	0.106

Then, the calculated accumulated displacement of solidification front and soft reduction efficiency are shown in Figure 12.

From Figure 12, it can be seen that the accumulated displacement of solidification front is increased from 0.238 mm to 0.805 mm, the total soft reduction efficiency decreases from 0.46 to 0.32. The total soft reduction efficiency is usually between 0.2 and 0.5 in actual production [14], the results of the model in this paper are in accordance with the total soft reduction efficiency zone.

The accumulated displacement of solidification front and the total soft reduction efficiency under different soft reduction amount are shown in Figures 13 and 14, respectively.

From Figure 13, it can be seen that the accumulated displacement of solidification front will be increased with increasing of total soft reduction amount, then, when the

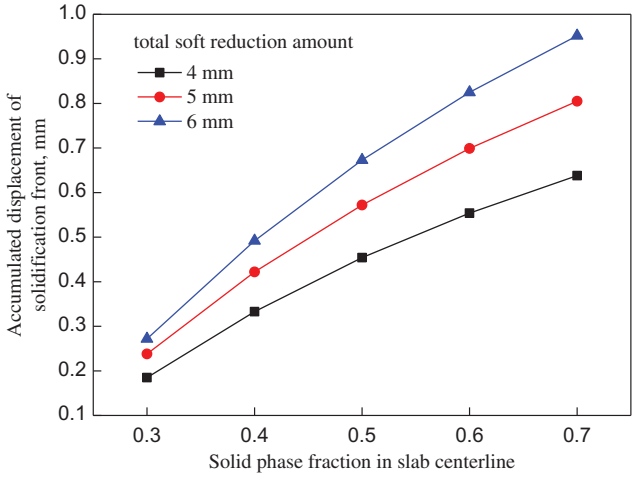

Figure 13: Relationship between accumulated displacement of solidification front and solid phase fraction in slab centerline.

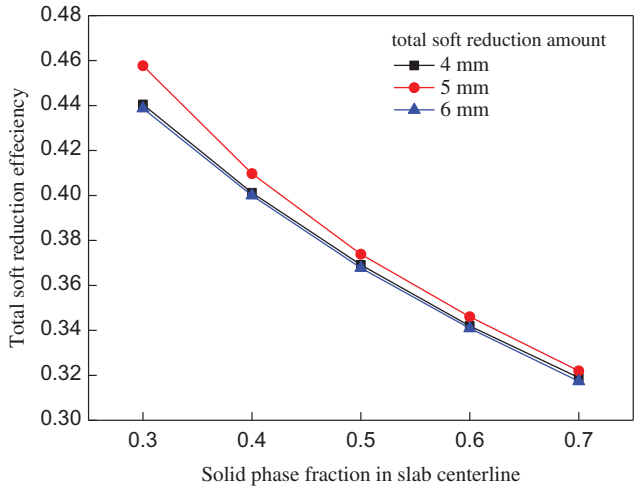

Figure 14: Relationship between total soft reduction efficiency and solid phase fraction in slab centerline.

shrinkage of solidification is larger, the total soft reduction amount should be larger. From Figure 14, it can be seen that the total soft reduction amount has little influence on the total soft reduction efficiency.

Conclusions

(1) The displacement along thickness direction of slab changes little in width center area under the same reduction amount, then it increases and a peak of deformation displacement appears in 0.075 m whose distance is far from the slab narrow face, finally, it decreases severely near the narrow face of slab.

(2) When the solid phase fraction in slab centerline keeps constant, the displacement of solidification shell toward to the width direction and thickness direction of slab increases with the increasing of reduction amount.

(3) The effective reduction efficiency decreases slightly with the increasing of reduction amount, when the solid phase fraction in slab centerline is 0.3, the effective reduction efficiency decreases from 0.463 to 0.436 when the reduction amount in reduction subzone is 0.15 mm and 0.25 mm, respectively, and the total reduction efficiency is changed very little when the total reduction amount is changed from 4 mm to 6 mm.

(4) When the reduction amount keeps constant, there is no obvious changes in the deformation displacement of solidification shell toward to the width direction of slab with increasing of the solid phase fraction in slab centerline, while the deformation displacement toward to the thickness direction of slab decreases, especially, the extent of that near the narrow face of slab decreases significantly.

(5) When the total reduction amount is 5 mm, the solid phase fraction varies from 0.3 to 0.7, the accumulated displacement of solidification front increases from 0.238 mm to 0.805 mm, the reduction efficiency decreases from 0.46 to 0.32.

Funding: This work was funded by the National Nature Science Foundation of China (No. 51474163 and No. 51504172).

References

[1] A. Scholes, Ironmaking Steelmaking, 32 (2005) 101–108.
[2] C.Q. Luo, H.W. Ni, G.M. Liu, et al., J. Iron Steel Res. Int., 15 (2008) 141–145.
[3] B. Wang, J.M. Zhang, C. Xiao, et al., High Temp Mater Processes, 35 (2016) 269–274.
[4] S. Josef, R. Pavel and K. Jaroslav, Material. Tehnol., 49 (2015) 725–729.
[5] S. Luo, M.Y. Zhu and C. Ji, Ironmaking Steelmaking, 41 (2014) 233–240.
[6] Q. Zhang, L.D. Yang and J. Tian, J. Iron Steel Res. Int., 15 (2008) 681–684.
[7] Z.W. Han, D.F. Chen and K. Feng, ISIJ Int., 50 (2010) 1637–1643.
[8] M.H. Wu, D. Josef and L. Andreas, Metall. Mater. Trans. A, 43A (2012) 945–964.
[9] Y. Gan and D.L. Chen, Iron Steel, 31 (1999) 27–31.
[10] Z.W. Lu and K.K. Cai, J. Univ. Sci. Technol. Beijing, 22 (2000) 303–306.
[11] Q.A. Chen, L.W. Liu and J.W. Wang, Iron Steel, 36 (2001) 44–46.
[12] S. Luo, M.Y. Zhu and C. Ji, J. Univ. Sci. Technol. Beijing, 32 (2010) 890–894.
[13] C.G. Cheng, J. Shuai, L. Yu, et al., J. Wuhan Univ. Sci. Technol., 34 (2011) 81–85.
[14] Y. Ito, A. Yarnanaka and T. Watanabe, Rev. Métall., 97 (2000) 1771–1176.